Mechanical behaviors of extruded Mg alloys with high Gd and Nd content

Xu, Yuling; Wang, Shiwei; Wang, Yuye; Chen, Li; Yang, Lixiang; Xiao, Lu; Yang, Li; Hort, Norbert

Published in:
Progress in Natural Science: Materials International

DOI:
10.1016/j.pnsc.2021.06.005

Publication date:
2021

Document Version
Publisher's PDF, also known as Version of record

Progress in Natural Science: Materials International 31 (2021) 591–598

Contents lists available at ScienceDirect

Progress in Natural Science: Materials International

journal homepage: www.elsevier.com/locate/pnsmi

Original Research

Mechanical behaviors of extruded Mg alloys with high Gd and Nd content

Yuling Xu [a,b,*], Shiwei Wang [b], Yuye Wang [b], Li Chen [b], Lixiang Yang [b,c], Lu Xiao [b], Li Yang [d], Norbert Hort [c,**]

[a] Chongqing Academy of Science and Technology, Chongqing, 401123, China
[b] Shanghai Spaceflight Precision Machinery Institute, Shanghai, 201600, China
[c] MagIC-Magnesium Innovation Center, Helmholtz-Zentrum Geesthacht, 21502, Geesthacht, Germany
[d] College of Materials Science and Engineering, Chongqing University, Chongqing, 400045, China

ARTICLE INFO

Keywords:
Wrought Mg alloy
Mechanical properties
Rare earth element

ABSTRACT

The influence of alloying elements and heat treatment on the microstructure and mechanical behaviors of extruded Mg–Gd–Nd ternary alloys was investigated in this study. The grain sizes dramatically decreased after extrusion, and the particles which distributed in Mg matrix had great effect on the grain size. The grain sizes of extruded alloys decreased from 26 to 5 μm with the alloying content increasing. The mechanical test results show that both Gd and Nd had positive effect on the hardness, yield strength and Young's modulus. The ultimate tensile strength (UTS) was enhanced by Gd content, decreased with Nd content. The elongation of alloys was lower with higher alloying elements. Those extruded alloys were aged for 200 h in 200 °C. The Young's moduli were decreased by ageing treatment. Combined with microstructure study, the part of the reinforcement which identified as $Mg_5(Gd/Nd)$ was dissolved in Mg matrix. Nd element obviously has influence on the solubility of Gd in Mg alloys.

1. Introduction

Since mid of 1950s, rare earth elements (REs) were added in Mg–Zn series alloys to adjust mechanical properties. Then, a number of Mg–RE alloys were developed and introduced into the industry during past decades, such as WE43 (Mg–4wt.%Y–3wt.%RE (Nd, Gd) –0.5 wt%Zr), WE54 (Mg–5wt.%Y–4wt.%RE (Nd, Gd)–0.5 wt%Zr), EV31 (Mg–3wt.% Nd–1wt.%Gd–0.5 wt%Zr), etc. [1,2]. Those alloys normally have two or more REs and present outstanding creep-resistant and mechanical properties at both room and elevated temperature [3–5]. Large number of researches was carried out for systematic investigation on Mg–RE alloys. Among the REs, Gd and Nd draw increasing concern due to their high performance. Gd has high solid solubility in Mg, with a maximum solubility of 4.41 at.% at the eutectic temperature [6]. Gd has been proved to have higher solid solution strengthening effect compare with other alloy elements, such as Al, Zn, Y, etc. [7]. Additionally, Gd exhibits a strong age-hardening, and the β' phase greatly improve strength of Mg alloys [8,9]. On the other hand, Nd shows negligible solubility in Mg. The maximum solubility of Nd in solid Mg is 0.63 at.% at eutectic temperature [10,11]. However, the mechanical properties of Mg with Nd alloy are improved by age-hardening [12,13].

Recently, some researches focus on the Mg–heavy RE–light RE alloy systems, e.g., Mg–Gd–Y, Mg–Gd–Nd, Mg–Dy–Nd, etc., which have higher strength and creep resistance. Zheng et al. [14,15] reported that the effect of pre-deformation and ageing treatment on the microstructure and mechanical properties of Mg–11Gd–2Nd–0.4Zr alloy. The result showed that the strength of the alloy increased with increasing pre-deformation level, and the UTS are above 300 MPa between room temperature (RT) to 250 °C. Negishi et al. [16] systemically investigated the arrange of Mg–xGd/Dy–yNd alloys (here x = 3–9 wt% and y = 1–7 wt%). The solubility of Nd limits the Gd or Dy shift largely to lower concentration than those of Mg–Gd/Dy binary alloys. Peng et al. [13] studied the effect of Nd on microstructures, age-hardening behavior, and the mechanical properties of the Mg–8Gd–0.6Zr–xNd alloys. The addition of Nd significantly improved the mechanical properties and age hardening behavior of Mg–8Gd–0.6Zr–xNd alloys. More researchers paid attention on quaternary or more alloys, e.g., Mg–Gd–Y–Nd, Mg–Dy–Gd–Nd, and the interaction of the alloying elements became much more complex [9,17–19]. However, little research has been reported on the extruded Mg–Gd–Nd alloy with high alloy concentration. The combined effects of

* Corresponding author.
** Corresponding author.
E-mail addresses: sharlin_xu@hotmail.com (Y. Xu), norbert.hort@hzg.de (N. Hort).

https://doi.org/10.1016/j.pnsc.2021.06.005
Received 24 September 2020; Received in revised form 30 May 2021; Accepted 9 June 2021
Available online 25 June 2021

Table 1
Chemical composition of studied alloys.

Alloys	Abbreviation [25]	Elements content/at.%		
		Gd	Nd	Mg
Mg–10Gd–2 Nd	VND102	1.62	0.34	98.04
Mg–10Gd–5 Nd	VND105	1.61	0.92	97.47
Mg–15Gd–2 Nd	VND152	2.60	0.45	96.95
Mg–15Gd–5 Nd	VND155	2.59	1.04	96.37

Gd and Nd element on their solid solubility in Mg matrix and mechanical properties of alloys have not been investigated. And hence carrying out a systematic investigation on Mg–Gd–Nd alloys is necessary.

In the present study, a comparative study on the high REs content Mg alloy with Gd and Nd additions, four Mg alloys were extruded to bars. Those alloys were aged for 200 h at 200 °C. The microstructures of Mg alloys before and after ageing were observed, respectively. The elastic moduli, hardness, tensile/compression properties were investigated to in-depth understanding the effects of alloy elements and ageing treatment on the microstructure and mechanical properties of Mg–Gd–Nd alloys.

2. Materials and experimental procedures

Four Mg–Gd–Nd ternary alloys were prepared in this study. The cast processing was reported in previous publication [20]. The chemical compositions of all alloys were analyzed by A PerkinElmer 7300DV inductively coupled plasma atomic emission spectrometer (Table 1). All alloys were solid solute heat-treated at 530 °C for 16 h before extrusion. The billets were quenched in water (18 °C) immediately after the heat treatment.

Extrusion was performed at Fachgebiet Metallische Werkstoffe in TU Berlin, Germany. The cylindrical billets were machined to 93 mm in diameter and 200 mm in length. Those billets were preheating treated at 440 °C in an electromagnetic induction furnace for 30 min. The hot extrusion was performed at 450 °C with an extrusion ratio of 60:1, and the extrusion rate (the speed of the extruded bar at the die exit) was set at 0.6 mm/s. Those extruded Mg–Gd–Nd alloys were aged (T5 state) for 200 h at 200 °C followed by air-cooling.

The metallographic specimens for microstructure observations were etched in a solution of 8 g picric acid, 5 mL acetic acid, 10 mL distilled water and 100 mL ethanol after mechanical polishing. A FEI QUANTA 450 (FEI Company, Hillsboro, USA) scanning electron microscope (SEM) equipped with energy dispersive X-ray (EDS) analyzer was further used to observe the microstructure at an accelerative voltage of 20 kV. EDS was used to analyze the compositions of different phases with a minimum live time of 50 s. Transmission electron microscopy (TEM) investigation was conducted using a Tecnai G2 F20 S-TWIN operated at 200 kV quipped with Super-X energy dispersive spectroscopy (EDS). TEM foils from the extruded and T5 state VND155 alloys after aging treatment were prepared by twin-jet electro-polishing at 50 V using a solution of 10% perchloric acid and 90% ethanol cooled to −30 °C.

Vickers hardness, Young's modulus, tension and compression tests were measured for the as-extruded and T5 state alloys. Young's moduli of Mg alloys were measured with the impulse excitation technique using a resonant frequency and damping analyzer (RFDA, IMCE, Belgium) with a sample dimension of 6 × 7 × 45 mm^3. The hardness measurement was carried out using a Vickers hardness testing machine (KARL FRANK GmbH) with a load of 5 kg and a dwell time of 10 s [21]. An average of 10 measurements was made for each specimen to ensure the reproducibility of the results. The tension and compression tests were performed at room temperature using a Zwick 050 testing machine (Zwick GmbH & Co., KG, Ulm, Germany) according to DIN EN ISO 6892–1 [22] and DIN 50106 [23], respectively. The tensile specimens had a 30 mm gauge length, 6 mm diameter, and threaded heads. The compressive specimens were cylinders of height 16.5 mm and diameter 11 mm. Both tension and compression tests were done under a strain rate of 1×10^{-3} s^{-1}. Three parallel specimens were taken for each group.

Phase composition and content were calculated using the CALPHAD (Calculation of Phase Diagrams) method in Thermo-Calc Software with version 4 of TCMG4 magnesium-based alloy database [24].

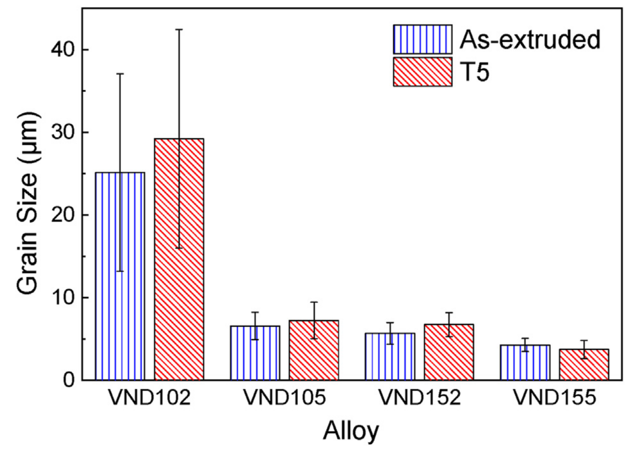

Fig. 1. Average grain size of Mg–Gd–Nd alloys.

3. Results

The average grain size of studied alloys is presented in Fig. 1. One can see that the grains dramatically decreased with increasing of alloy content. For VND102 alloy the grain size reached to 25 μm, and increased to 30 μm after T5 treatment. The average grain sizes of other three alloys (VND105, VND152, and VND155) were around 5 μm, and had little change by T5 treatment.

Fig. 2 shows the SEM images of studied Mg–Gd–Nd alloys. VND102 alloy shown highly different microstructure compared with other three alloys. Only a few white particles with regular blocky shape were found in as-extruded VND102 alloy (Fig. 2(a)). However, in other three alloys, these are large number of particles disturbed in Mg matrix with two different sizes. Some white particles with larger size, 5–10 μm in size, occupied entire grains (Fig. 2(b, c, d)). Small particles, 0.5–2 μm in size, were observed both in the grains and on the grain boundary. After ageing at 200 °C for 200 h, many thin precipitates with bright contrast were observed along the grain boundary (arrows in Fig. 2). However, the larger size particles volume became smaller after T5 treatment.

The phases composition calculated by Thermo-Calc Software is listed in Table 2. The XRD patterns obtained from the as-extruded Mg–Gd–Nd alloys are shown in Fig. 3. According to the simulation result, the extruded alloys with lower Nd at 450 °C contained Mg_5RE phase and little $Mg_{41}RE_5$ phase. Comparing between VND105 and VND155 alloy, Gd content had great influence on the phase composition. In VND105 alloy the Mg_5RE and $Mg_{41}RE_5$ phase were 1.99 and 7.21 mol%, respectively. With Gd content increasing to 2.6 at.%, the alloy contained much higher Mg_5RE phase reaching to 10.17 mol%, and $Mg_{41}RE_5$ phase decreased to 5.74 mol%. The simulation results were in good agreement

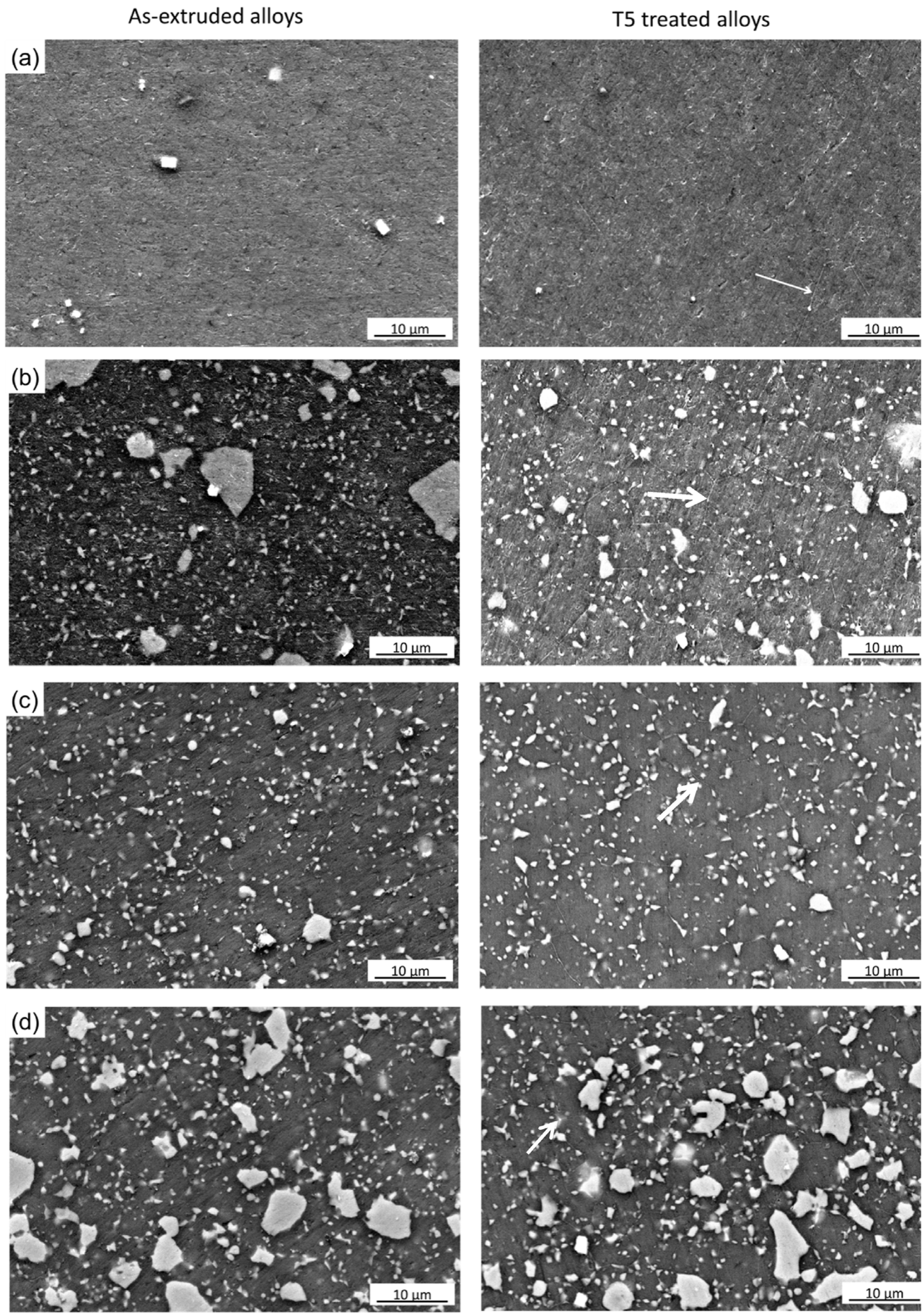

Fig. 2. SEM images of extruded Mg–Gd–Nd alloys:
(a) VND102; (b) VND105; (c) VND152; (d)VND155.

with the XRD results. Only Mg_5RE phase and α-Mg with lower Nd were observed in the alloys. However, after ageing treatment, large amount of solid solutes precipitated from Mg matrix, and more Mg_5RE phase formed. The Mg_5RE phase concentration increased to 8 and 15 mol% in the alloys content 1.6 at.% and 2.6 at.% Gd, respectively.

The typical microstructures of as-extruded and aged VND155 observed by TEM are shown in Fig. 4 and Fig. 5, respectively. The EDX test results show that those particles contained 7–9 at.% Gd and 4–6 at.%

Table 2
Phases composition and content for Mg–Gd–Nd systems.

Alloy	Temperature [°C]	α_{hcp} [mol%]	Mg_5RE [mol%]	$Mg_{41}RE_5$ [mol %]
VND102	200	90.35	8.53	1.12
	450	97.22	2.45	0.33
	530	100	–	–
VND105	200	84.73	8.27	7.00
	450	90.80	1.99	7.21
	530	95.26	–	4.74
VND152	200	83.92	15.78	0.30
	450	90.30	9.70	–
	530	93.67	6.33	–
VND155	200	78.20	15.51	6.29
	450	84.09	10.17	5.74
	530	88.42	8.31	3.27

Nd (Fig. 4(b)). According to the electron diffraction patterns recorded from the particle P1 (Fig. 4(c)) and P2 (Fig. 4(d)), the large size and fine particles can both be identified as the Mg_5RE phase (F 43 m, a = 2.2 nm) [26,27]. Many plate-shaped β' precipitates were clearly visible in grains and show dark contrasts (Fig. 5(a, d, e)) [28,29]. The precipitate observed on the grain boundary was also tested as Mg_5RE phase (Fig. 5(c)). It was identified by performing EDX analysis and the results indicated that it has highly Gd (9.92 at %) content (Fig. 5(b)).

Besides, the evolution of the grain boundary structure showed two different microstructures. The grain boundaries were apparent in TEM images in Fig. 6. From Fig. 6(a), it can be clearly seen that the β' precipitates crossed the grain boundary without precipitates. However, another microstructure consisted of two constantaneous procedures (Fig. 6(b)), i.e., growth of grain boundary precipitates (GBPs) and widening of precipitate free zones (PFZs). The PFZs also formed between the large size particles and β' precipitates. The PFZ was about 90 nm wide at the grain boundary, while increased to over 150 nm at large size particles. With the variation of the orientation between grain boundary and electron beam, the GBPs were found to exhibit linear or dispersive arrangement along grain boundaries.

The hardness and Young's modulus test result of as-extruded and T5 state alloys are presented in Fig. 7(a). The hardness values increased from 77 to 98 kg mm^{-2} with increasing of alloy elements. All the Vickers hardness data of aged alloys were increased by ~20–35 kg mm^{-2}. However, the T5 treatment showed different effect on the Young's moduli of those alloys. According to the test results (Fig. 7(b)), the Young's modulus was increased from 46.67 to 47.34 GPa by increasing of the alloy element concentration. The Young's moduli of all T5 state alloys decreased after ageing.

Fig. 8(a) and (b) reveal the tensile and compression properties of Mg alloys at room temperature, respectively. The tensile yield strength (TYS) and compressive yield strength (CYS) of as-extruded alloys had a roughly rising trend with increasing alloying concentration. The ageing treatment showed great positive effect on the TYS and CYS. Especially for VND102 alloy, the CYS of T5 state alloy increased 170 MPa, from 165 MPa to 335 MPa. Moreover, VND152 alloys after T5 treatment had the highest TYS and CYS in four alloys, which reached to 313 MPa and 345 MPa, respectively. It was found that VND152 also had much better ultimate tensile strength (UTS) and ultimate compressive strength (UCS) than the rest of alloys in this study. The values difference of the UTS was small except VND102, and the UCS of VND152 and VND155 also had little differences. The elongation and compressibility had a downtrend with increasing alloying elements. With increasing of alloy concentration, the values of the elongation of as-extruded alloys decreased from 20% to 11%. However, the values of the elongation of as-extruded alloys were significantly higher than that of T5 state alloys, while the compressibility of as-extruded alloys was lower.

4. Discussion

The solubility of Gd in Mg can reach 23 wt% (4.53 at.%) at eutectic temperature (542 °C) [6]. According to previous study the Gd atoms could be completely dissolved in the Mg matrix for Mg15Gd alloy [30]. For Mg–Gd–Nd ternary alloys, the solubility of Gd atoms is obviously limited by the existence of Nd. Thus, more Gd will exist in second phase, and hence the concentrations of Gd are high in both small and big particles after extrusion. A careful comparison between the alloys with different Nd contents shows that the Mg_5RE phase with the larger volume was more likely to exist in the higher Nd content alloys (Fig. 2(b) and (d)). Combining with the previous microstructure of the Mg–Gd–Nd alloy before extrusion, it ca(b)n be concluded that these large particles are formed by extruding and crushing the interdendritic compound after solution treatment. Moreover, the extrusion temperature of 450 °C was lower than the solid-solution temperature of 530 °C, which causes another part of Gd and Nd to emerge from the matrix, and therefore the small particles of Mg_5RE phase formed on the grain boundary area.

Earlier study result show that alloy content, e.g., solid solute elements and precipitate, had great influences on the Young's modulus of alloys [31]. The Young's modulus can be predicted by changing the composition of the alloys. The results of this study also confirm the conclusion, i.e., the Gd solid solutes and second phases had positive effect on the Young's modulus of Mg alloys. The Young's moduli of extruded Mg–Gd–Nd alloys increased with increasing of Gd and Nd concentration. The β' phase

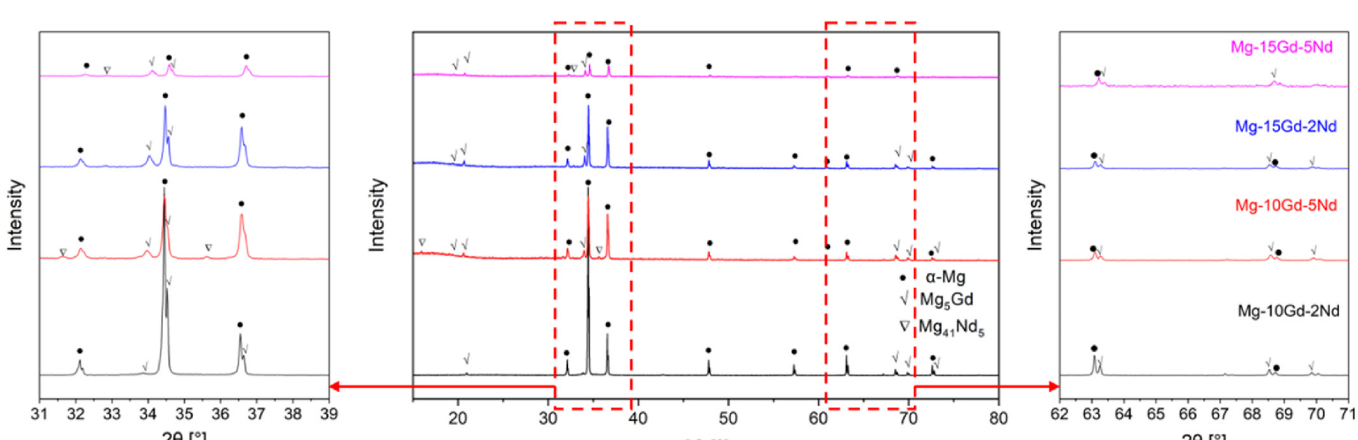

Fig. 3. XRD patterns of as-extruded Mg–Gd–Nd alloys.

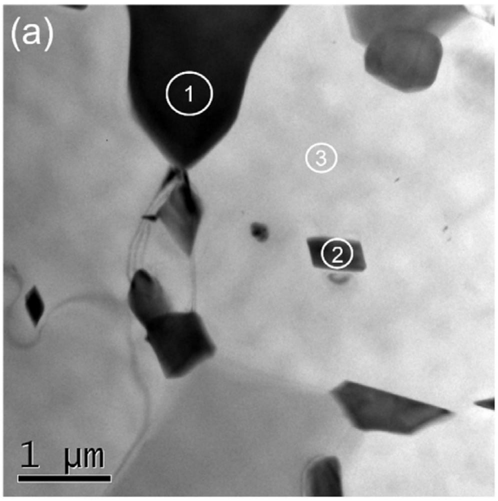

(b)

Point No.	Element content [at.%]		
	Mg	Gd	Nd
1	85.50	8.89	5.59
2	98.54	1.28	0.16
3	87.53	7.69	4.76

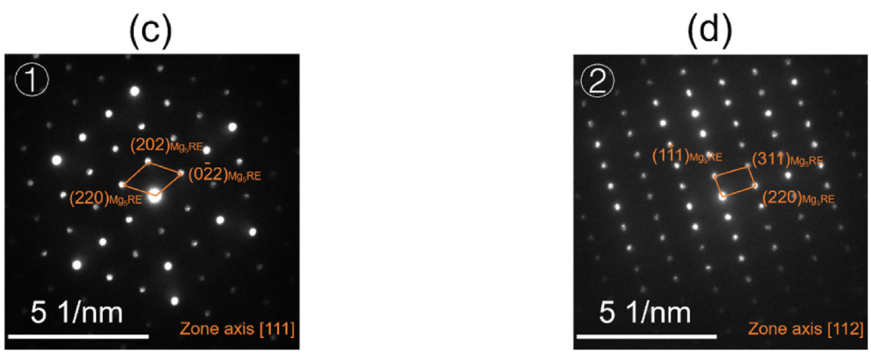

Fig. 4. TEM analysis of as-extruded VND155 alloy: (a) TEM micrograph; (b) EDX analysis; (c) and (d) electron diffraction patterns of the particles.

precipitated and distributed after ageing treatment could greatly enhanced the Young's moduli of Mg alloy. However, the fact that Young's moduli decreased in this case means that part of intermetallic is reduced after aging, and the positive contribution of β' phase have not enough capital to cover the negative influence on the Young's moduli.

The result of TEM test indicate that the alloy aged at 200 °C for 200 h and with the content amount of Mg_5RE phase is favorable for precipitation at grain boundary. It has been found that PFZs existed between the Mg_5RE and β' phases. The continuous precipitation in the grains may not be the whole of the precipitation process. Another obvious change in the microstructure during aging is the preferential precipitation of the equilibrium phase along the grain boundary of Mg alloy matrix, accompanied by the formation of no precipitation zone. In order to reduce the free energy, the metastable precipitates dissolve along PFZs and solute atoms diffuse to grain boundaries. Under this mechanism, GBPs and PFZs grow simultaneously with aging time [8,15].

Combined with the tensile and compression tests results, the ageing treatment obviously enhanced the yield strength, but decreased the elongation of those alloys. It may be related to the β' phase and PFZs. On the on hand, the fine precipitates provide precipitation strengthening effect for the yield strength. On the other hand, GBPs were more likely to cause the fracture from grain boundary, and the PFZs formed along grain boundary also leaded the intergranular fracture and deteriorated the mechanical properties. VND152 alloy showed highest ultimate strengths with more than 400 MPa. The T5 treatment had little effect on the strength, but greatly influenced the elongation of this alloy. However, compared with studies of Liu et al. [18], Li et al. [17], Zheng et al. [15] and Guan et al. [32], VND152 alloy had highest strength, which is owed to the Gd solid solutes and fine precipitates.

5. Summary

The mechanical behavior and microstructure of as extruded and aged Mg–Gd–Nd ternary alloys has been investigated. Under the combined action of Gd and Nd, the microstructure evolution and mechanical properties of Mg alloys are different from those of binary alloys.

1 The solid solubility of Gd is decreased by Nd adding in the Mg alloy. Large amount of Mg_5RE phases which contain high Gd still exist in Mg alloy matrix with 5 wt% Nd after extrusion at 450 °C. Part of the large Mg_5RE particles are dissolved by ageing treatment, but small Mg_5RE particles precipitate on the grain boundary. Large amount β' phases form in the grains after ageing.
2 The Young's moduli values increase with increasing of alloy elements for as extruded alloys. However, ageing treatment has negative effect on the Young's moduli. It is related to the reduction of Mg_5RE phase.
3 PFZs and GBPs form after ageing treatment, which has great influence on the mechanical properties. PFZs have been always found to exist in the area of GBPs, and they decrease the ductility of the alloys and make the alloy fragile.

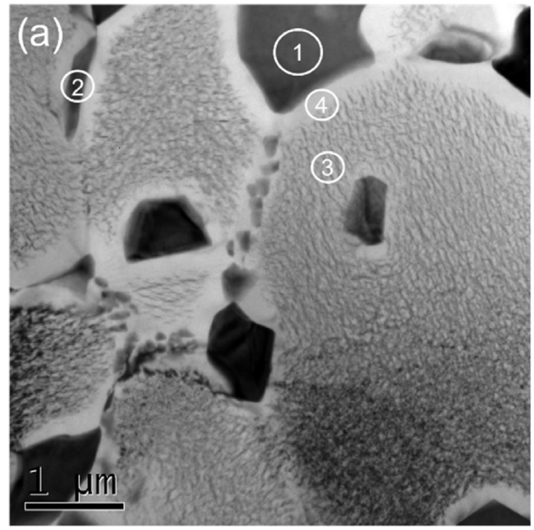

(b)

Point No.	Element content [at.%]		
	Mg	Gd	Nd
1	87.22	8.65	4.12
2	89.20	9.92	0.86
3	94.20	5.35	0.43
4	97.77	2.22	0

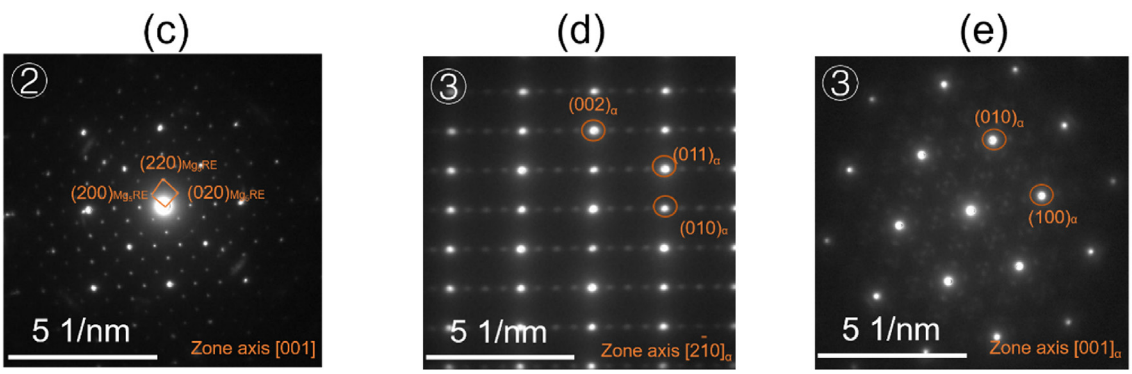

Fig. 5. TEM analysis of aged VND155 alloy: (a) TEM micrograph; (b) EDX analysis; (c), (d) and (e) electron diffraction patterns of the particles.

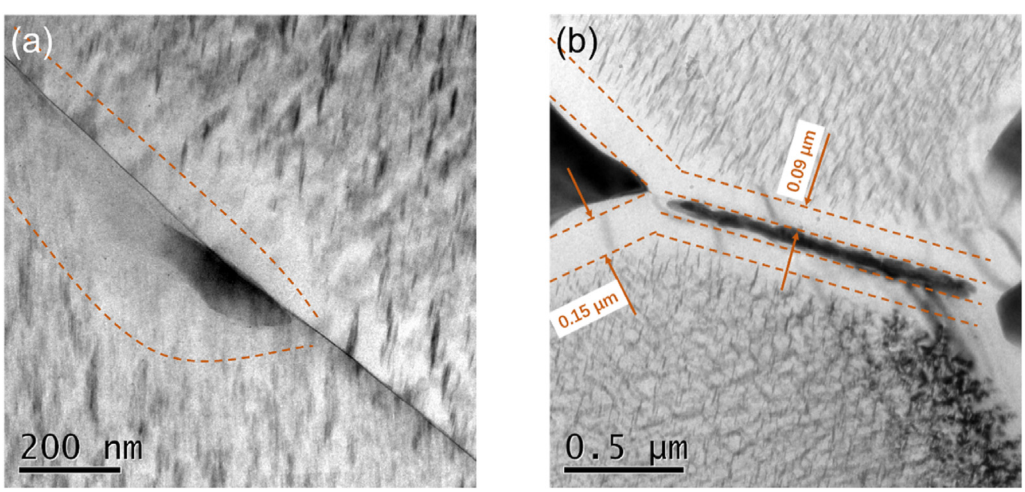

Fig. 6. TEM micrographs showing grain boundary structure.

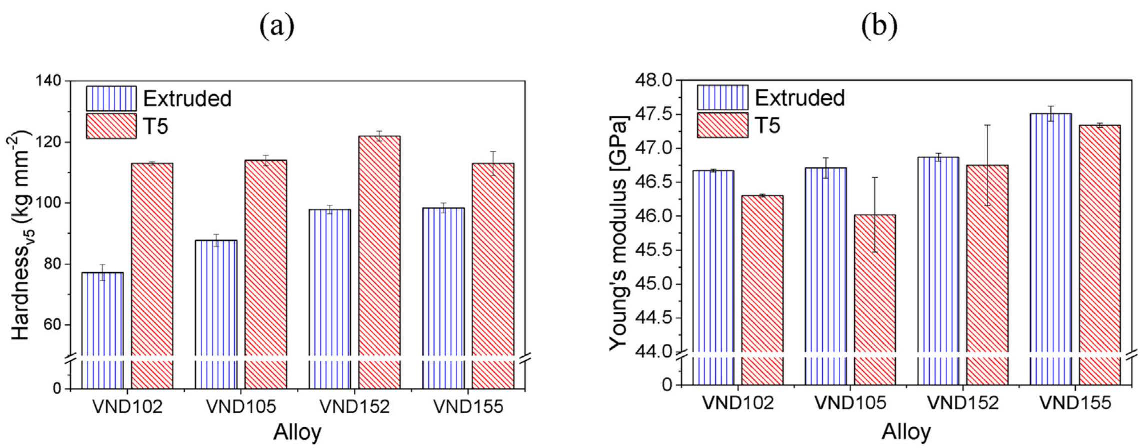

Fig. 7. (a) Hardness and (b) Young's modulus result of Mg–Gd–Nd alloys.

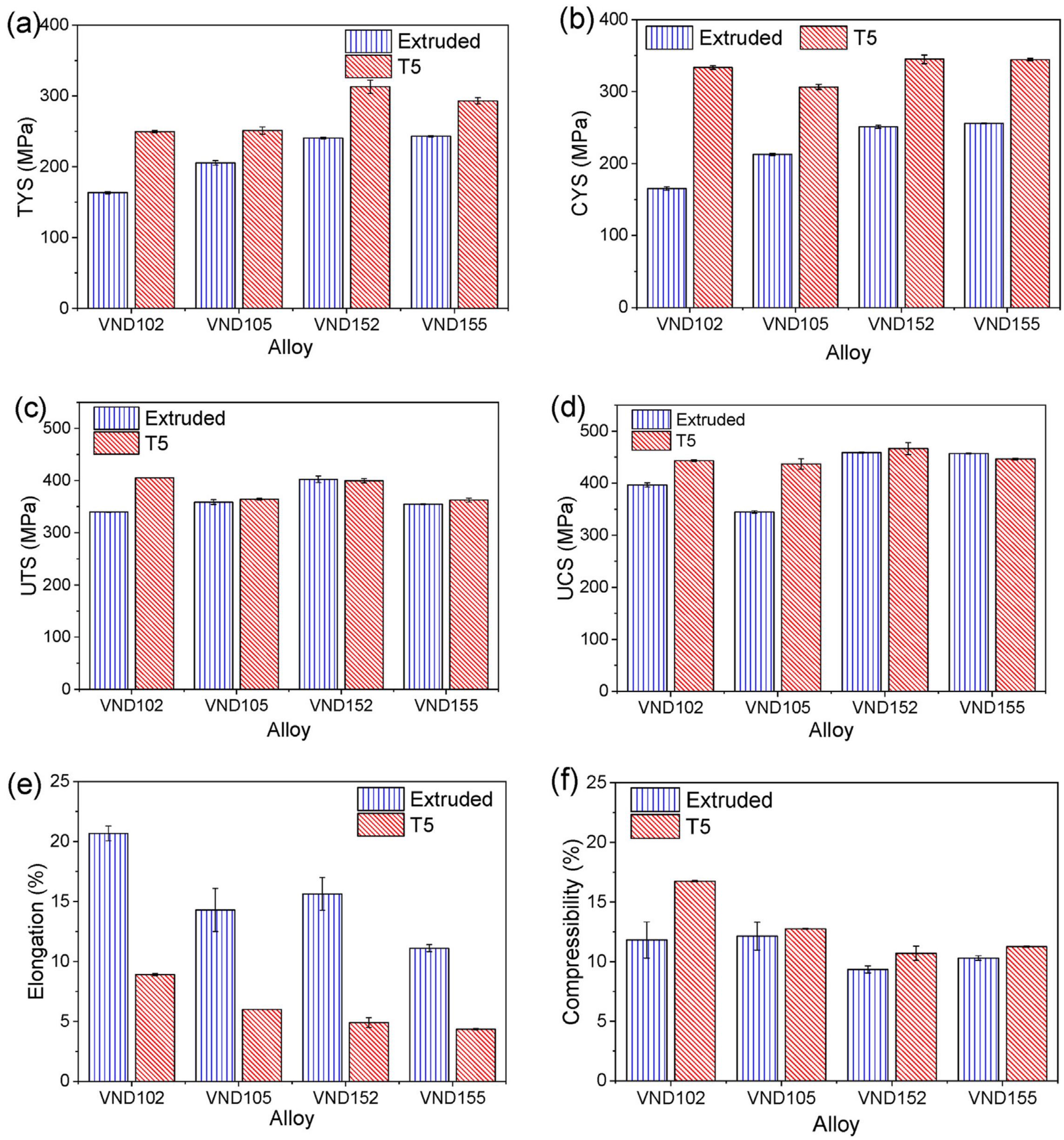

Fig. 8. Tensile and compressive properties of Mg–Gd–Nd alloys:
(a) tensile yield strength (TYS), (b) compressive yield strength (CYS), (c) ultimate tensile strength (UTS), (d) ultimate compressive strength (UTS), (e) elongation, (f) compressibility (strain at maximum stress point).

Declaration of competing interest

The authors declare that they have no known competing financial interests or personal relationships that could have appeared to influence the work reported in this paper.

Acknowledgements

The authors would like to acknowledge the help of Mr. Günther Meister (HZG, Germany) during casting and heat treatment. The authors thank Prof. Walter Reimers (FMW, TU Berlin) for offering help of extrusion processing. The present work was co-supported by the China Postdoctoral Science Foundation (Grant No. 2020M673156), Shanghai Pujiang Program (Grant No. 20PJ1404900), and Science and Technology Commission of Shanghai Municipality (Grant No. 18511109300).

References

[1] K.K. Alaneme, E.A. Okotete, J. Magnes. Alloys 5 (4) (2017) 460–475.
[2] H. Friedrich, B. Mordike, Springer, Berlin, 2006.
[3] K.U. Kainer, Y.D. Huang, H. Dieringa, N. Hort, Materials Science Forum, Trans Tech Publ, 2010, pp. 73–80.
[4] J. Song, J. She, D. Chen, F. Pan, Journal of Magnesium and Alloys 8 (1) (2020) 1–41.
[5] J. Bohlen, S. Yi, D. Letzig, K.U. Kainer, Mater. Sci. Eng. 527 (26) (2010) 7092–7098.
[6] L.L. Rokhlin, CRC Press LLC, London, UK, 2003.
[7] L. Gao, R.S. Chen, E.H. Han, J. Alloys Compd. 481 (1–2) (2009) 379–384.
[8] Y. Zhang, W. Rong, Y. Wu, L. Peng, J.F. Nie, N. Birbilis, J. Alloys Compd. 777 (2019) 531–543.
[9] J.H. Li, G. Sha, T.Y. Wang, W.Q. Jie, S.P. Ringer, Mater. Sci. Eng. 534 (2012) 1–6.
[10] Y.M. Savitskii, V. Terekhova, I. Novikova, Zh. Neorg. Khim. 3 (9) (1958) 2138–2142.
[11] J. Yan, Y. Sun, F. Xue, S. Xue, W. Tao, Mater. Sci. Eng. 476 (1–2) (2008) 366–371.
[12] S. Gorsse, C.R. Hutchinson, B. Chevalier, J.F. Nie, J. Alloys Compd. 392 (1–2) (2005) 253–262.
[13] Q. Peng, Y. Wu, D. Fang, J. Meng, L. Wang, J. Mater. Sci. 42 (11) (2007) 3908–3913.
[14] K.Y. Zheng, J. Dong, X.Q. Zeng, W.J. Ding, Mater. Sci. Eng. 491 (1–2) (2008) 103–109.
[15] K.Y. Zheng, J. Dong, X.Q. Zeng, W.J. Ding, Mater. Sci. Eng. 489 (1–2) (2008) 44–54.
[16] Y. Negishi, T. Nishimura, S. Iwasawa, S. Kamado, Y. Kojima, R. Ninomiya, J. Jpn. Inst. Light Metals 44 (10) (1994) 555–561.
[17] Y. Li, K. Zhang, Y. Zhang, X. Li, M. Ma, Rare Met. 29 (3) (2010) 317–322.
[18] X. Liu, Z. Zhang, Q. Le, L. Bao, Journal of Magnesium and Alloys 4 (3) (2016) 214–219.
[19] L. Qiuzu, D. Xiaofeng, L. Yanping, W. Xiaojia, J. Alloys Compd. 690 (2017) 961–965.
[20] Y. Xu, L. Yang, W. Liu, J. Sun, L. Xiao, X. Jiang, N. Hort, Magnesium Technology (2020) 79–85.
[21] Standard Test Methods for Rockwell Hardness of Metallic Materials, ASTM, USA, 2017.
[22] Metallic Materials - Tensile Testing - Part 1: Method of Testing at Ambient Temperature, DIN, Germany, 2017.
[23] Testing of Metallic Materials - Compression Test at Room Temperature, DIN, Germany, 2016.
[24] A.J. Ondersson, T. Helander, L. Höglund, P.F. Shi, B. Sundman, Calphad 26 (2002) 273–312.
[25] Standard Practice for Codification of Certain Nonferrous Metals and Alloys, Cast and Wrought, ASTM, USA, 2004.
[26] X. Chen, Y. Zhang, L. Peng, C. Zhang, Calphad 48 (2015) 43–54.
[27] D. Li, J. Dong, X. Zeng, C. Lu, W. Ding, J. Alloys Compd. 439 (1–2) (2007) 254–257.
[28] H. Liu, W. Xu, N. Wilson, L. Peng, J. Nie, J. Alloys Compd. 712 (2017) 334–344.
[29] A. Issa, J.E. Saal, C. Wolverton, Acta Mater. 83 (2015) 75–83.
[30] Y. Xu, F. Gensch, Z. Ren, K.U. Kainer, N. Hort, Prog. Nat. Sci.: Materials International 28 (6) (2018) 724–730.
[31] Y.L. Xu, J. Li, Z.Y. Zhong, K.U. Kainer, H. Norbert, Magnesium Technology (2017) 341–347. Springer2018.
[32] L. Guan, Y. Deng, H. Shi, L. Yang, M. Chen, J. Mater. Eng. Perform. 27 (1) (2017) 243–252.